Practical Radiation Oncology (2012) **2**, 122–137

practical radiation oncology
pro
www.practicalradonc.org

Original Report

Dosimetric evaluation of a "virtual" image-guidance alternative to explicit 6 degree of freedom robotic couch correction

Vikren Sarkar PhD[a], Brian Wang PhD[a], Jacob Hinkle BS[b], Victor J. Gonzalez MD[c], Ying J. Hitchcock MD[a], Prema Rassiah-Szegedi PhD[a], Sarang Joshi PhD[a,b], Bill J. Salter PhD[a,*]

[a]*Department of Radiation Oncology, University of Utah, Salt Lake City, Utah*
[b]*Scientific Computing and Imaging Institute, University of Utah, Salt Lake City, Utah*
[c]*Department of Radiation Oncology, University of Arizona, Tucson, Arizona*

Received 5 March 2011; revised 1 July 2011; accepted 21 July 2011

Abstract

Purpose: Clinical evaluation of a "virtual" methodology for providing 6 degrees of freedom (6DOF) patient set-up corrections and comparison to corrections facilitated by a 6DOF robotic couch.

Methods: A total of 55 weekly in-room image-guidance computed tomographic (CT) scans were acquired using a CT-on-rails for 11 pelvic and head and neck cancer patients treated at our facility. Fusion of the CT-of-the-day to the simulation CT allowed prototype virtual 6DOF correction software to calculate the translations, single couch yaw, and beam-specific gantry and collimator rotations necessary to effectively reproduce the same corrections as a 6DOF robotic couch. These corrections were then used to modify the original treatment plan beam geometry and this modified plan geometry was applied to the CT-of-the-day to evaluate the dosimetric effects of the virtual correction method. This virtual correction dosimetry was compared with calculated geometric and dosimetric results for an explicit 6DOF robotic couch correction methodology.

Results: A (2%, 2mm) gamma analysis comparing dose distributions created using the virtual corrections to those from explicit corrections showed that an average of 95.1% of all points had a gamma of 1 or less, with a standard deviation of 3.4%. For a total of 470 dosimetric metrics (ie, maximum and mean dose statistics for all relevant structures) compared for all 55 image-guidance sessions, the average dose difference for these metrics between the plans employing the virtual corrections and the explicit corrections was −0.12% with a standard deviation of 0.82%; 97.9% of all metrics were within 2%.

Conclusions: Results showed that the virtual corrections yielded dosimetric distributions that were essentially equivalent to those obtained when 6DOF robotic corrections were used, and that always outperformed the most commonly employed clinical approach of 3 translations only. This suggests

A portion of this work was presented in an oral presentation at the 52nd Annual Meeting of the American Society for Radiation Oncology in San Diego, CA.

Conflicts of interest: This work was performed with partial support from a Siemens Grant.

* Corresponding author. Department of Radiation Oncology, Huntsman Cancer Hospital, 1950 Circle of Hope, Salt Lake City, UT 84112.
E-mail address: bill.salter@hci.utah.edu (B.J. Salter).

1879-8500/$ – see front matter
doi:10.1016/j.prro.2011.07.005

that for the patient datasets studied here, highly effective image-guidance corrections can be made without the use of a robotic couch.

Introduction

An ever increasing emphasis on conformal, hypofractionated delivery schemes continues to focus attention on the importance of high precision image-guided delivery techniques. Over the past decade, many capable image-guided approaches have emerged, including stereotactic ultrasound guidance,[1] stereoscopic planar imaging,[2,3] in-room CT-on-rails (CTOR),[4-7] on-board cone beam CT imaging,[8-15] 3-dimensional (3D) video surface rendering,[16] and electromagnetic tracking of embedded transponders.[17-19] All of these guidance techniques share a single, simple goal of facilitating accurate repositioning of the targeted volume to account and correct for interfractional or intrafractional target motion.

Each of the previously mentioned methods can use in-room-acquired spatial information about the target location to derive the 3 translations and 3 rotations required to return the target to the originally simulated position and orientation on which the treatment plan is based. After derivation of the required 6 degrees of freedom (6DOF) corrections, the clinical user is tasked with implementing the corrective changes using translational shifts of the treatment couch and, if possible, rotational corrections as well. Because typically equipped treatment couches only posses the ability to perform 1 of the 3 rotational components of 6DOF corrections (ie, couch "yaw," or coronal plane rotation), typical users are currently forced to choose between correcting for the 6 degrees of error using less than 6 degrees of correction, or some users are now upgrading their treatment couches to third party add-on "robotic" couches that have recently become available with 6DOF correction capability.[20-22] In addition to translational error correction, these 6DOF robotic couches are typically capable of correcting for angular errors on the order of 3 degrees or less in pitch (ie, rotation in the sagittal plane), roll (ie, rotation in the axial plane), and yaw orientations. Upgrades entail replacement of the linear accelerator (linac) treatment couch top assembly with a robotically driven couch top assembly and the cost for such upgrades typically ranges from $250,000 to $500,000. Because of the limited availability of funds for such major equipment upgrades, it is not surprising that only a small subset of available clinical linacs have been upgraded with 6DOF robotic correction capability to date.

Recently, an interesting new idea for 6DOF image-guided correction was presented by Bose et al.[23] The strategy they presented entailed corrections applied not to the patient, but to the treatment beam orientation; as defined by gantry rotation, collimator rotation, and treatment couch yaw rotation. Perhaps the most attractive aspect of this proposal is that, if viable, such a strategy would make 6DOF corrective strategies available to virtually all clinical users without the need for major hardware upgrades, as nearly all commercially available linacs possess the inherent ability to perform such corrections. In their original work, Bose et al[23] described and demonstrated the mathematical methodology that could be used to calculate the 3 couch translations and beam-specific gantry and collimator rotations, in combination with a single couch yaw, necessary to correct for patient misalignment and misorientation, and they presented a proof of principle clinical example.

While the methodology and proof of principle work presented by Bose et al[23] are quite interesting and, potentially, of significant clinical value, the only way to assess the true viability of this "virtual" 6DOF correction would be to explore or test numerous clinical examples in an image-guided environment.

In this work, we use 3D fan beam CT image-guided datasets acquired using an in-room CT-on-rails (CTOR) system (SOMATOM Sensation 40; Siemens Healthcare, Erlangen, Germany) to explore the clinical viability of the virtual 6DOF correction proposed by Bose et al.[23] We investigate 55 different CTOR image-guided datasets from 11 different patients with either head and neck (H&N) or pelvic disease sites. We use these 55 CT "datasets of the day" to calculate the dose distributions that would have been delivered had the virtual 6DOF correction method been employed to correct for image-guidance errors, and we compare this to the calculated dose distributions that would have been achieved if a 6DOF explicit correction had been employed by using a robotic couch. We perform geometric analysis, dose-volume histogram (DVH) analysis, and dosimetric gamma analysis comparison of both approaches and, in doing so we assess the clinical viability of this potentially important new image-guidance correction strategy, relative to the current gold standard of explicit correction by robotic couch.

Materials and methods

Experiment design overview

We evaluated the viability of the virtual 6DOF image-guidance correction strategy described by Bose et al[23] (ie, 3 translations plus rotational correction by adjustment of gantry, collimator, and single couch yaw rotation[s]) by comparing it with the results that are achieved when using an explicit 6DOF spatial correction strategy achieved with a 6DOF robotic couch. Rather than comparing only the

geometry of relevant structures, we chose to also focus on comparison of the post-correction DVHs and dose distributions as we believe these to be the most important metrics for comparison. The overall experimental design was to use in-room CTOR datasets acquired for image guidance of individual patients, taken immediately prior to a particular treatment fraction, and calculate the isodose distributions that would be achieved after corrective shifts were implemented using each of the 2 described correction strategies. We then compared the geometry and dosimetry obtained using each of the 2 methods to determine whether the virtual correction strategy yielded results that were comparable with the current standard of explicit robotic couch correction.

Bose method; Brief overview

We now briefly describe the virtual correction approach previously presented by Bose et al.[23] The inputs to the algorithm are the 3 translations and 3 rotations derived from the rigid 6DOF registration between the image set of the day and the planning image dataset. While the software allows for performing an automatic registration based on any one of several available algorithms, in the interest of maintaining consistency with a standard clinical approach we performed all registrations manually, under the guidance and final approval of the physician.

Using the results of the 6DOF registration, the system calculates a so-called "ideal" polygon, created by the intersection of each planned beam (or beamlet, for the case of intensity modulated radiation therapy [IMRT]) with the isocentric plane. The method next randomly generates a "proposed" set of 3 translations, a single couch-yaw rotation, and beam-specific gantry and collimator rotations for consideration. The corresponding polygon for each beam's intersection with the isocentric plane is then calculated. Next the Euclidian distance between the edges of the "ideal" polygon and the "proposed" polygon for all segments in the plan are calculated. This process is iterated until the Euclidian distance between the ideal and proposed polygons for all segments is minimized, and this represents the final solution. For a more complete and mathematical description of the process, the reader is referred to the original publication by Bose et al.[23]

Patient dataset selection

A total of 11 patient image-guided datasets were retrospectively chosen for this study; 5 with H&N disease and 6 with pelvic malignancies. All patients had been imaged on our in-room 40 slice, large-bore Siemens CT-on-rails (CTOR) immediately prior to treatment, with at least 5 different CTOR image-guidance sessions performed during the course of each patient's treatment. For purposes of this study, the first 5 consecutive CTOR image-guidance datasets for each patient were selected, for a total of 55 unique CTOR image-guidance datasets. Table 1 lists the treatment modality as well as prescription dose for all 11 patients studied here.

Table 1 Summary of treatment modality and prescription dose for each patient used as part of this study

Case	Treatment modality	Prescription dose (Gy)
Pelvic case 1	IMRT	50.4
Pelvic case 2	IMRT	45.0
Pelvic case 3	IMRT	50.4
Pelvic case 4	IMRT	45.0
Pelvic case 5	IMRT	50.4
Pelvic case 6	IMRT	45.0
H&N case 1	IMRT	67.5
H&N case 2	IMRT	54.0
H&N case 3	IMRT	67.5
H&N case 4	3DCRT	60.0
H&N case 5	IMRT	67.5

3DCRT, 3-dimensional conformal radiotherapy; H&N, head and neck; IMRT, intensity modulated radiation therapy.

6DOF image registration process and determination of explicit 6DOF corrections

The first step performed to determine image-guided explicit 6DOF corrections (ie, X,Y,Z translations and couch pitch, roll, and yaw rotations) is to register the "image set of the day" taken immediately prior to treatment, to the reference image set (eg, CT simulation dataset). As mentioned previously, we used fan beam CT datasets acquired on an in-room CTOR system for acquisition of all image-guidance datasets used here and we registered these to the CT datasets generated at time of simulation on our 16 slice GE LightSpeedRT scanner (GE Health Care, Waukesha, WI). CTOR datasets were acquired using a slice thickness of 2 mm and pixel dimension 0.98 mm × 0.98 mm and GE LightSpeed datasets were acquired using a slice thickness of 2.5 mm and pixel dimension 0.98 mm × 0.98 mm. For purposes of image registration, we used the Siemens Adaptive Targeting II software (AT II), which is a new, preclinical version of the currently released Adaptive Targeting I software (AT I). The rationale for using the preclinical AT II software was that the AT I software only allows for a 3D, translation-only registration, while the newer AT II software allows the user to perform a full 6-dimensional registration that includes the 3 translations and also the 3 rotations that best align the image-guidance dataset to the simulation (reference) CT dataset. The AT II software is meant to run at the linac treatment console system and subsequently reports the 6DOF corrections that are required to achieve the just-performed image registration.

Because the software is currently available only as a research tool, we used an anthropomorphic phantom

(RANDO Phantom; The Phantom Laboratory, Salem, NY) to independently verify the geometric accuracy of the software registration process. To test for accuracy of translation, CT scans of the pelvic and H&N regions of the phantom were obtained. Then the phantom was rescanned after known translational shifts were applied in all 3 cardinal directions. The 2 (original and shifted) CT datasets were manually registered and the resulting software-derived shifts were calculated and compared with the known shifts. Similarly, to test for accuracy of software-derived rotations, the baseline image datasets were rotated known amounts, about a known point using in-house software. The rotated and original image sets were then manually registered using the AT II software and the software-derived rotations were compared with the known rotations. All software-derived translations were seen to agree within 1 mm, or approximately 1 voxel, of known translations. All software-derived rotations were seen to agree within 0.5 degree.

To perform 6DOF image registrations, the simulation CT and structures, along with the treatment plan were sent as DICOM objects to the AT II station. Prior to the acquisition of the daily image-guidance images, the patient was positioned to the treatment isocenter. For purposes of CT visualization of the setup isocenter location, three 1-mm BBs were placed in triangulation on the patient for treatment isocenter localization and the CTOR dataset was acquired. This is analogous to the methodology reported previously by Shiu et al.[5] The location of the BBs was then used within the AT II software to identify the imaging isocenter in the CTOR image-guidance dataset, and this imaging isocenter represented the "origin" about which all rotational and translational corrections were reported by the software. All fusions were carefully reviewed for accuracy by the responsible physician, and the 6DOF spatial correction parameters reported by the AT II software were recorded for later use in calculating the isodose distributions that would have resulted from use of an explicit 6DOF correction strategy by robotic couch.

For comparison with what is standard practice at many institutions that do not possess a robotic couch, we also performed a separate registration where we only allowed for translations. This registration was also reviewed and approved by the physician who approved the 6DOF fusion and was used to provide a comparison of what would happen if we were to correct for patient positioning using a translations only strategy.

Determination of virtual 6DOF corrections

The AT II software also includes a new module that allows for calculation of the optimal X,Y,Z translations along with gantry, collimator, and single couch yaw rotation(s) as described for virtual 6DOF correction by Bose et al.[23] This module was employed to calculate and record the required virtual 6DOF corrections (ie, 3 translations and gantry, collimator, and single couch yaw rotation[s]) for later use in calculating dose distributions that would have resulted from the virtual 6DOF correction strategy.

Evaluation of geometric accuracy of the virtual corrections compared with the explicit corrections

In order to visually assess the degree to which the virtual correction approach reproduces the beam-to-anatomy geometry produced by an explicit robotic couch correction, we identified a set of fiducial points (stable, very reproducible anatomical landmarks) that could be identified from CT, relative to individual treatment fields, once all corrections were applied (by either the virtual or explicit approach). This digitally reconstructed radiography (DRR)-based assessment was performed for 2 cases; the H&N and pelvic cases which demonstrated the worst dosimetric agreement between virtual and explicit correction approaches (ie, fraction 4 of pelvic case 6, and fraction 5 of H&N case 2; see the following section (Plan comparison through dose statistics and DVH analysis). Two fiducial points were localized for each case, with points intentionally chosen to be located at the edges of the target or high-dose region. Thus, we were evaluating a truly worst case scenario for geometric agreement between the virtual and explicit approaches, in that we performed the evaluation for the 2 cases which experienced the worst levels of dosimetric agreement and we intentionally chose fiducial points that were at the periphery of the high-dose region, thus maximizing the impact of rotation-induced translations of the fiducial point. We note that, in order to validate the reproducibility of identifying the fiducial point locations, we conducted an experiment wherein we identified a total of 4 different points, a minimum of 5 times each, and determined the standard deviation in the x, y, and z coordinates of the points. There was no case where the standard deviation exceeded 0.2 mm (ie, < 1 voxel) in any of the 3 cardinal directions.

For both comparison cases, the DRR-based coordinates of each fiducial point location for the explicit approach was compared with the corresponding coordinates from DRRs generated using plans corrected using the virtual approach to assess how closely the fiducial point locations agreed geometrically. For each fiducial point, we then calculated the 3D vector difference between the beam-relative location of the fiducial point in the plan employing the virtual approach versus the location in the explicit correction robotic plan. Due to the fact that, in the end, the dose distribution for a particular treatment plan is dependent on contributions from all fields, the average of the 3D vector displacements from all fields of each treatment plan was compared as a means to assess the geometric correspondence of the 2 methods. Low values for the mean composite 3D vector differences would indicate that the virtual correction strategy was effectively

mimicking the geometric correction afforded by a 6DOF robotic correction approach. Lastly, in order to provide additional context and perspective, we also collected and present the same information for the "translations only" approach as well as the "zero corrections" approach.

Calculation of isodose distributions for 6DOF explicit correction strategy

To calculate the dose distributions that would result from an explicit robotic couch correction we would need to either perform the explicit spatial corrections in the treatment room using a robotic couch, and then re-image the patient, or we could use the CT image-set-of-the-day obtained prior to correction, and then digitally rotate and translate the dataset as if the spatial corrections had been performed. As we do not currently have a robotic couch that can perform the rotational corrections in the vault and because, even if we did have a robotic couch, the former approach would require administration of additional, unneeded imaging dose, we chose the latter "digital" approach.

In order to perform a rigid transformation of the CT scan, a C++ program was written using the ITK library (http://www.itk.org). The DICOM CTOR series was read as a 3D volume, and rotation of the 3D volume was implemented using trilinear interpolation. The resulting volume was then output as a DICOM series using ITK. So that DVH analysis could later be performed, the attending physician who originally delineated target and critical structures on the original treatment planning (simulation) CT dataset also contoured relevant structures on each CTOR dataset of the day. For the pelvic cases, bladder, rectum, and small bowel were contoured. Because the node-based target volume was believed to be constant throughout the treatment course, the original planning target volume was copied forward to the image- set-of-the-day after appropriate fusion of the 2 datasets was performed. For the H&N cases, because the target volume is known to change throughout treatment, we did not include the target volume in our analysis. Structures that were recontoured for the H&N cases include the spinal cord, the left and right parotids, and the mandible.

In order to implement rotation of the structures, it was necessary to produce a set of contours which represented the same enclosed volume but at the re-sampled CT slice locations. This was accomplished through another C++ program written using the VTK library (http://www.vtk.org). The algorithm read the structure file format and used the list of contours for each structure to create a triangular mesh representation of the entire structure. This structure was then transformed by rotating the associated vertices and triangle's normal vectors. The transformed structure was then "re-sliced" at all the resampled slice locations and the resulting polygons were exported as contours. The resulting structures could then be imported back into the treatment planning software (Eclipse version 8.8; Varian Medical Systems, Palo Alto, CA) along with the rotated CT scan to accurately represent the patient and relevant contours in rotated orientation; as if the 6DOF corrections had been applied and the patient re-imaged. The entire methodology was tested with phantom datasets of various geometries and readily identifiable high-contrast borders to confirm accurate representation of the rotated CT and contour datasets.

After the rotated CT data and structures were imported into the Eclipse treatment planning system, the originally designed, unmodified treatment beams were applied to the plan and isodose distributions which were representative of what would result from employing an explicit image-guidance position correction strategy were calculated.

Calculation of isodose distributions for 6DOF virtual correction strategy

In order to calculate isodose distributions for the virtual correction strategy we imported the uncorrected CT-of-the-day dataset along with previously described, physician-defined relevant structures into the eclipse treatment planning system. The originally designed treatment plan parameters were then applied to the CT-of-the-day, but with isocenter modified to correct for X,Y, Z translations and beam specific gantry angle, beam specific collimator angle, and single couch yaw modified to correct for rotations, as determined by the previously described Bose et al[23] virtual correction module contained in the AT II software.

Additional calculated treatment plans

For the purposes of added context, or reference, we also calculated treatment plan isodose distributions representing a situation wherein no image-guided corrective shifts were applied (zero correction strategy), and treatment plan isodose distributions representing the commonly employed clinical approach wherein only 3 translational (X,Y,Z) corrections are made (translations only correction strategy). These isodose distributions were both calculated on the CT-image-set-of-the-day with either no modification to the original plan parameters (zero correction strategy) or with isocenter relocated according to the 3 translational shifts recorded from the AT II software (see previous section on "6DOF image registration process and determination of explicit 6DOF corrections") for 3DOF spatial correction (translations only correction strategy). Thus, 4 total isodose distributions were calculated: (1) zero correction strategy; (2) translations only correction strategy; (3) explicit correction strategy (ie, robotic couch correction); and (4) virtual correction strategy (ie, Bose et al[23] methodology), for each of the 55 image-guided datasets, representing 220 total recalculated isodose distributions for comparison.

Plan comparison through dose statistics and DVH analysis

Treatment plans for explicit, virtual, zero correction, and translations only correction strategies were directly compared through dosimetric statistics, including the maximum and mean doses to all delineated structures, as well as through comparison of the dose-volume histograms (DVHs) for all structures. For the pelvic cases, this entailed evaluation of tumor coverage as well as dose to the bladder, rectum, and small bowel. For the H&N cases, dose to the left and right parotids, mandible, and spinal cord were compared.

Plan comparison through gamma analysis

In order to gain additional insight into how the entire dose distribution from each of the correction strategies compared with what is obtained when using an explicit robotic correction strategy, a gamma analysis,[24] identical to that commonly used to compare predicted IMRT dose distributions to delivered distributions, was performed. Using in-house-developed software, the dose distribution from the plan using explicit corrections was read together with the dose distribution that was to be compared with it. The analysis involved computing the 2D gamma of all points receiving a dose greater than 10% of the prescription dose for each slice within the calculated dose distribution. The analysis software then provided the percentage of all points from all slices that had a gamma value of 1 or less.

The gamma analysis was performed using criteria (3%, 3mm), (2%, 2mm), (2%, 1mm), and (1%, 1mm) for the virtual, translation only, and zero correction datasets, relative to the explicit correction strategy, for all 55 image guided datasets, thus representing 660 individual gamma analysis comparisons with the explicit correction method.

Results

Table 2 summarizes the mean and maximum corrective translations and rotations derived from the full 6DOF registrations performed on the AT II system, as well as the mean and maximum couch, collimator, and gantry rotations performed while applying the virtual corrections. We note that the highest couch-yaw correction needed for all 55 cases investigated here was 2 degrees and, because only coplanar beams were used for the 11 patients we explored, a 2 degree of couch yaw was not enough to lead to collisions in any of the cases. However, we acknowledge that if the virtual approach were to be used clinically, in particular for non-coplanar situations, a check of clearance for larger couch-yaw situations might be deemed prudent. We further note that even though standard limitations on currently available robotic couch solutions are on the order of 3 degrees maximum rotational correction in any cardinal rotational plane, we calculated explicit robotic corrections assuming that the robotic couch was capable of fully correcting these larger rotations. The assumption was that, if needed, the patient could have been repositioned or re-setup to reduce the rotations to within the 3-degree corrective capability of typical robotic couches, but it is worth noting that the virtual correction approach is not necessarily limited in this regard and would, therefore, not require such patient repositioning.

Evaluation of the geometric accuracy of the virtual corrective strategy

Figures 1 and 2 present the previously discussed, DRR-based beams eye view geometric comparisons of 3 different beams each, from both the H&N and pelvic cases, respectively, which showed the worst agreement based on dosimetric comparisons (ie, fraction 4 of pelvic case 6, and fraction 5 of H&N case 2; see Materials and Methods section [Plan comparison through dose statistics and DVH analysis]). Shown for each of the 3 beams represented in each case are the DRR with beam geometry and outline, isocenter location (circle at reticule coordinate system [0,0]) and both fiducial point locations (small "x" marks on each image). The corresponding fiducial "x" mark locations can be visually compared with each other for the explicit, zero correction, translations only, and virtual methods. What can be observed, in general, is that

Table 2 Summary of maximum and mean translations and rotations used for the explicit and virtual positioning corrections

	Translations			Explicit rotations			Virtual rotations		
	LR (mm)	SI (mm)	AP (mm)	Patient yaw (°)	Patient pitch (°)	Patient roll (°)	Couch yaw (°)	Collimator rotation (°)	Gantry rotation (°)
Pelvis max	8.0	8.0	18.0	1.0	7.0	2.0	1.0	7.0	2.0
Pelvis mean	2.3	4.3	7.1	0.5	2.6	1.0	0.5	1.8	1.0
H&N max	5.0	5.0	7.0	2.0	5.0	4.0	2.0	5.0	4.0
H&N mean	2.4	2.1	1.9	1.0	1.5	1.9	1.0	1.0	0.9

AP, anterior-posterior; H&N, head and neck; LR, left-right; max, maximum; SI, superior-inferior.

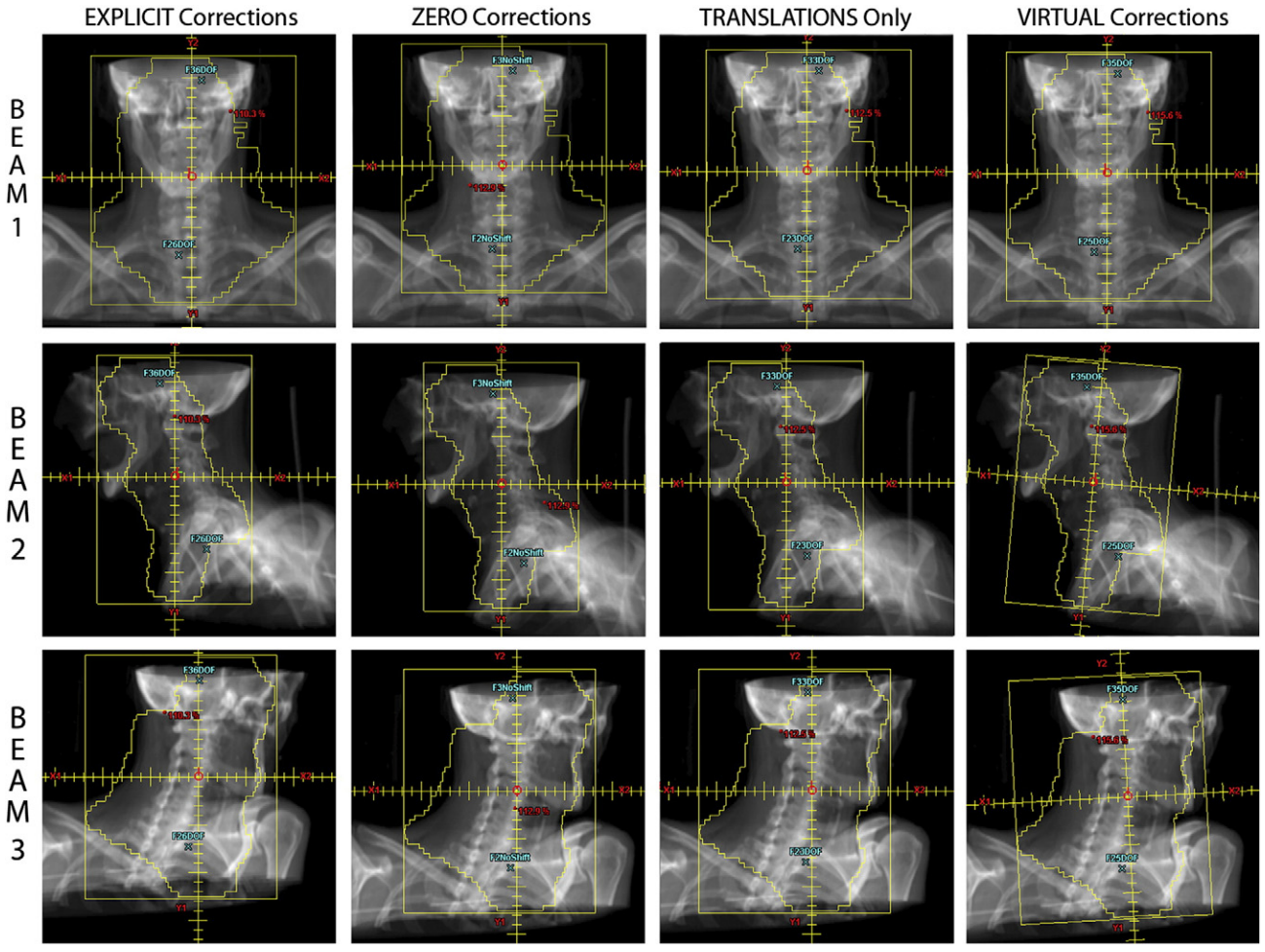

Figure 1 Example from one of the head and neck cases showing digitally reconstructed radiographs from plans using the explicit, zero corrections, translations only, and virtual corrective strategies to determine the geometric effect of the different strategies on the location of fiducial points from a beam's eye view perspective.

the relationship between the fiducial locations and the beam geometry and underlying anatomy for the zero correction and translations only approaches result in the largest geometric differences when visually compared with the explicit approach, with the virtual approach coming closest to reproducing the beam-to-fiducial geometry of the explicit robotic correction approach. Table 3 summarizes the results of the 3D-vector composite differences for geometric accuracy of the virtual corrective strategy when compared with the explicit correction strategy and, for the sake of comparison, we also present the results for the translations only strategy that is routinely used in radiotherapy centers today. Because the 3D-vector composite difference represents the difference in the fiducial point's location relative to the position it would have been in when an explicit corrective strategy is used, small 3D-vector differences indicate that the strategy being considered performed well in correcting for positioning errors relative to the explicit robotic approach. The data from Table 3 shows that, in terms of overall 3D distance, the differences between the fiducial point coordinates are much greater for the translations only approach than for the virtual corrections approach, when each is compared against the explicit corrections approach (ie, the gold standard). In terms of percentage reduction of the 3D difference vector, we can calculate from Table 3 that the virtual correction approach reduces the geometric error of the commonly employed translations only approach by an average of 76.0% (minimum = 53.9%; maximum = 86.1%) and that the average worst case difference vectors are 2.2 mm and 1.0 mm for the pelvis and H&N, cases, respectively (maximum = 3.0 mm and 1.0 mm, respectively).

Comparison of corrective strategies using dosimetric statistics

Table 4 shows the percent differences between the dosimetric metrics calculated for the explicitly corrected 6DOF plan compared with the virtually corrected 6DOF plan for the H&N cases, while Table 5 shows the analogous results for the pelvic cases. All differences are

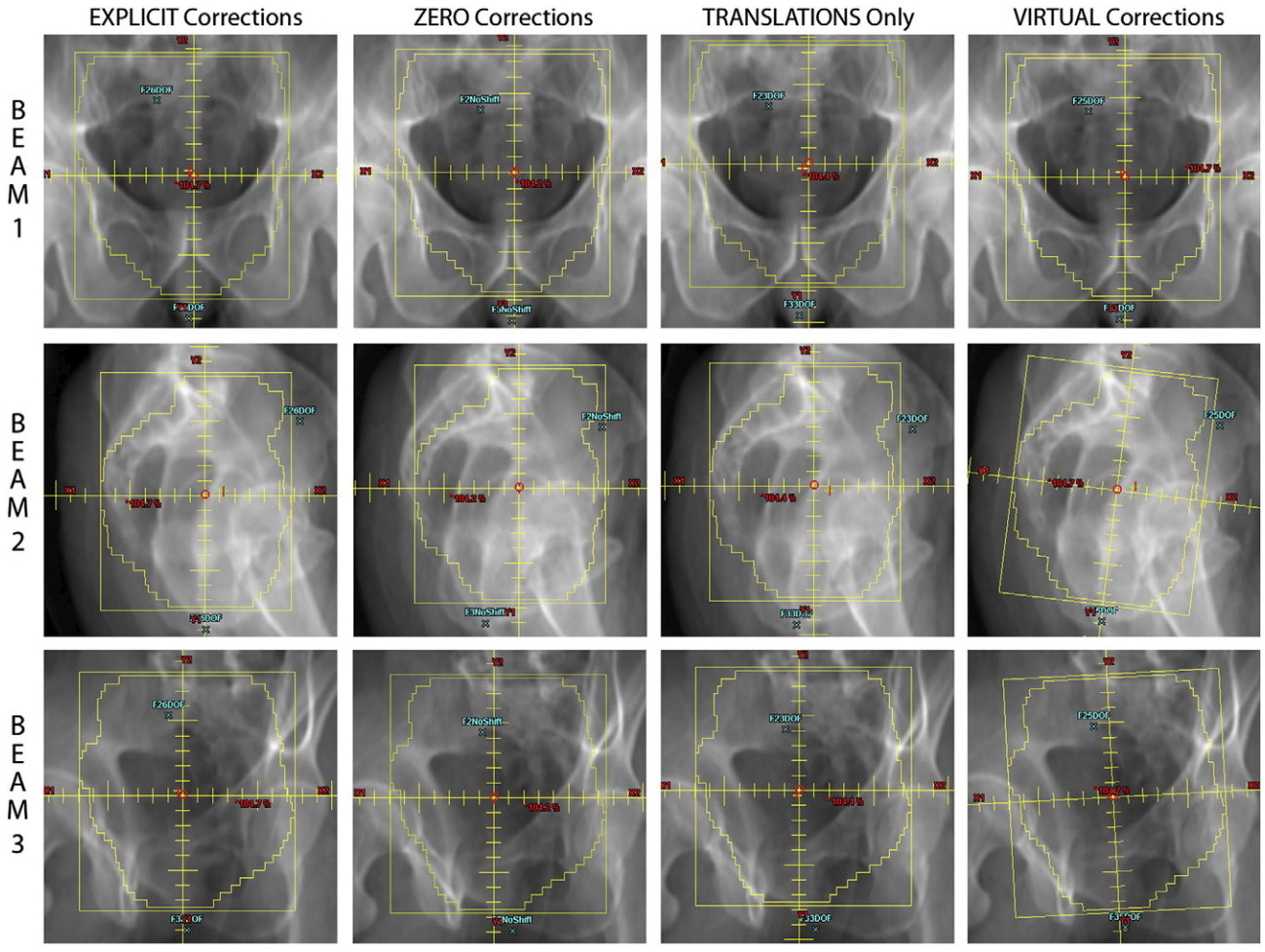

Figure 2 Example from one of the pelvic cases showing digitally reconstructed radiographs from plans using the explicit, zero corrections, translations only, and virtual corrective strategies to determine the geometric effect of the different strategies on the location of fiducial points from a beam's eye view perspective.

as a percentage of the prescribed target dose, with differences greater than 2% being bolded. The metrics evaluated in this study include maximum and mean doses for relevant critical structures and planning target volumes. The tables show that, even with a very tight tolerance threshold of 2% applied, there are only 10 statistical metrics out of a total of 470 where the difference exceeded 2%. The mean difference across all patients and all image-guidance sessions was −0.12% ± 0.82%, thus indicating that the virtual correction strategy yielded target and organ

Table 3 Summary of 3D distance between fiducials when the translation only or virtual corrective strategies are used compared with the same fiducial location when the explicit corrections are made

Case	Fiducial 1		Fiducial 2	
	Translations only approach 3D Δ vector (mm)	Virtual correction approach 3D Δ vector (mm)	Translations only approach 3D Δ Vector (mm)	Virtual correction approach 3D Δ vector (mm)
Worst case pelvis	6.5	3.0	9.1	1.4
Worst case H&N	7.2	1.0	4.9	1.0

The distance reported is the average of distances calculated individually from each field and the smaller the distance, the more successful was that corrective strategy at geometrically positioning the point at the same final location as applying the explicit strategy. Note that the translations only 3D Δ vector is larger in all cases compared with the virtual correction approach, thus indicating that the virtual correction approach performed better in spatially reorienting the fiducial points relative to the 7 fields of each treatment plan. On average, the virtual correction approach reduces the geometric error of the commonly employed translations only approach by an average of 76.0%.
3D, 3-dimensional; H&N, head and neck.

Table 4 Percent dose differences between the metrics calculated for the explicitly corrected plan versus the virtually corrected plan for each of 5 fractions of the 5 head and neck patients (ie, 25 image-guidance sessions).

Patient 1

	Lt Parotid	Lt Parotid	Rt Parotid	Rt Parotid	Cord	Cord	Mandible	Mandible
	Max	Mean	Max	Mean	Max	Mean	Max	Mean
FX1	0.30	−0.70	0.70	−0.70	−0.30	0.80	0.60	0.00
FX2	0.60	−0.70	−0.10	1.90	−1.10	0.00	−0.20	0.60
FX3	−0.90	−0.70	−0.40	−0.70	−1.70	0.80	−0.40	−0.20
FX4	−1.50	−1.20	0.70	0.60	−0.40	0.20	0.50	0.80
FX5	0.50	−1.40	−0.30	−0.30	−1.70	0.80	0.10	0.00
MEAN	−0.20	−0.94	0.12	0.16	−1.04	0.52	0.12	0.24
ST. DEV	0.94	0.34	0.54	1.11	0.68	0.39	0.43	0.43

Patient 2

	Lt Parotid	Lt Parotid	Rt Parotid	Rt Parotid	Cord	Cord	Mandible	Mandible
	Max	Mean	Max	Mean	Max	Mean	Max	Mean
FX1	−0.10	0.40	−1.40	0.30	−0.70	−0.10	−0.20	0.10
FX2	0.30	0.20	−1.20	0.10	−0.60	0.00	0.00	−0.20
FX3	−0.60	−0.60	−1.60	1.80	−0.90	0.00	1.20	0.00
FX4	−0.60	0.20	−1.10	1.00	0.80	0.20	−1.30	0.20
FX5	−1.80	0.20	**−5.30**	**2.70**	−0.70	−0.20	−1.60	0.40
MEAN	−0.56	0.08	−2.12	1.18	−0.42	−0.02	−0.38	0.10
ST. DEV	0.79	0.39	1.79	1.08	0.69	0.15	1.12	0.22

Patient 3

	Lt Parotid	Lt Parotid	Rt Parotid	Rt Parotid	Cord	Cord	Mandible	Mandible
	Max	Mean	Max	Mean	Max	Mean	Max	Mean
FX1	−1.20	−0.30	−1.10	−0.70	−0.40	0.20	−0.40	−0.50
FX2	−1.10	−1.90	1.50	1.10	−1.90	0.10	0.10	0.10
FX3	−1.90	−1.70	−0.90	0.60	−1.20	0.20	−0.40	0.40
FX4	−0.30	−0.70	0.90	1.10	−0.10	0.30	−0.50	0.10
FX5	0.80	−0.20	0.10	1.30	−1.70	0.20	−0.10	0.20
MEAN	−0.74	−0.96	0.10	0.68	−1.06	0.20	−0.26	0.06
ST. DEV	1.03	0.79	1.12	0.81	0.79	0.07	0.25	0.34

Patient 4

	Lt Parotid	Lt Parotid	Rt Parotid	Rt Parotid	Cord	Cord	Mandible	Mandible
	Max	Mean	Max	Mean	Max	Mean	Max	Mean
FX1	−1.50	−0.10	0.80	0.00	−0.60	0.10	0.60	0.60
FX2	−0.10	0.10	−0.10	0.30	−0.60	−0.20	−0.20	0.60
FX3	1.10	0.10	−0.90	−0.20	−0.20	0.00	−1.00	0.60
FX4	0.90	0.10	−1.20	−0.40	−0.10	0.30	−1.10	0.20
FX5	0.80	0.20	0.00	0.20	−0.80	0.00	0.10	0.50
MEAN	0.24	0.08	−0.28	−0.02	−0.46	0.04	−0.32	0.50
ST. DEV	1.08	0.11	0.79	0.29	0.30	0.18	0.73	0.17

Patient 5

	Lt Parotid	Lt Parotid	Rt Parotid	Rt Parotid	Cord	Cord	Mandible	Mandible
	Max	Mean	Max	Mean	Max	Mean	Max	Mean
FX1	−1.50	−1.50	0.30	−0.90	−2.00	0.70	−0.50	**−2.30**
FX2	−1.20	−1.80	−0.10	−1.80	0.90	0.70	1.20	**−2.20**
FX3	−0.70	−0.40	−0.20	−1.20	0.20	0.40	−1.30	**−2.60**
FX4	−1.90	−0.30	−0.10	−0.20	1.70	0.20	0.50	−0.90
FX5	−0.80	−0.60	−1.20	−0.70	0.90	0.60	−0.20	**−2.60**
MEAN	−1.22	−0.92	−0.26	−0.96	0.34	0.52	−0.06	**−2.12**
ST. DEV	0.50	0.68	0.56	0.59	1.41	0.22	0.96	0.70

All differences are as a percentage of the prescription dose, with those greater than 2% shown as boldface.

Table 5 Percent dose differences between the metrics calculated for the explicitly corrected plan versus the virtually corrected plan for each of 5 fractions of the 6 pelvic patients (ie, 30 image-guidance sessions)

Patient 1										Patient 2									
	PTV	PTV	PTV	Bladder	Bladder	Rectum	Rectum	Small Bowel	Small Bowel		PTV	PTV	PTV	Bladder	Bladder	Rectum	Rectum	Small Bowel	Small Bowel
	Max	Mean	V95	Max	Mean	Max	Mean	Max	Mean		Max	Mean	V95	Max	Mean	Max	Mean	Max	Mean
FX1	−0.20	0.10	0.13	0.10	0.20	0.00	−0.90	0.20	0.10	FX1	−0.10	0.20	0.41	−0.10	−0.60	−0.10	0.10	0.20	1.60
FX2	0.20	0.20	0.43	0.40	0.20	−0.50	0.10	0.30	−0.60	FX2	0.40	0.20	0.59	−0.20	−0.20	0.10	0.20	−0.20	1.30
FX3	0.40	0.20	0.19	0.20	0.30	0.00	0.10	0.50	0.00	FX3	0.50	0.30	0.64	0.30	0.00	0.50	0.30	1.50	1.50
FX4	−0.10	0.10	0.09	0.30	0.00	−0.50	0.00	−0.20	0.20	FX4	0.40	0.20	0.52	0.50	−0.40	0.10	0.10	−0.10	0.50
FX5	0.80	0.30		0.40	0.10	0.30	0.10	0.00	−0.80	FX5	0.30	0.20	0.44	0.30	0.20	0.40	0.20	−0.90	0.50
MEAN	0.22	0.18	0.20	0.28	0.16	−0.14	−0.12	0.16	−0.22	MEAN	0.30	0.22	0.52	0.16	−0.20	0.20	0.18	0.10	1.08
ST. DEV	0.40	0.08	0.13	0.13	0.11	0.35	0.44	0.27	0.45	ST. DEV	0.23	0.04	0.10	0.30	0.32	0.24	0.08	0.88	0.54

Patient 3										Patient 4									
	PTV	PTV	PTV	Bladder	Bladder	Rectum	Rectum	Small Bowel	Small Bowel		PTV	PTV	PTV	Bladder	Bladder	Rectum	Rectum	Small Bowel	Small Bowel
	Max	Mean	V95	Max	Mean	Max	Mean	Max	Mean		Max	Mean	V95	Max	Mean	Max	Mean	Max	Mean
FX1	0.30	0.30	0.41	0.20	0.20	0.40	0.10	1.20	−0.70	FX1	0.10	0.00	0.09	−0.10	0.00	0.20	0.00	0.00	−0.50
FX2	0.30	0.20	0.39	0.30	0.40	0.20	0.00	0.20	0.70	FX2	0.20	0.00	0.00	−0.40	−0.30	0.00	−0.10	−0.20	−0.50
FX3	0.10	0.30	0.52	0.00	0.40	−0.30	0.00	−0.30	0.10	FX3	−0.10	0.00	−0.01	−0.20	−0.10	0.10	−0.10	0.00	−0.20
FX4	0.30	0.30	0.53	0.40	0.60	0.20	0.30	0.00	−0.30	FX4	0.00	−0.10	0.08	−0.20	0.00	−0.10	−0.10	−0.30	−0.50
FX5	0.20	0.30	0.19	0.40	0.30	0.40	0.30	−0.60	−0.70	FX5	−0.10	0.00	0.09	−0.20	−0.10	0.00	0.00	0.00	0.00
MEAN	0.24	0.28	0.41	0.26	0.38	0.18	0.14	0.10	−0.18	MEAN	0.02	−0.02	0.05	−0.22	−0.10	0.04	−0.06	−0.10	−0.34
ST. DEV	0.09	0.04	0.14	0.17	0.15	0.29	0.15	0.69	0.59	ST. DEV	0.13	0.04	0.05	0.11	0.12	0.11	0.05	0.14	0.23

Patient 5										Patient 6									
	PTV	PTV	PTV	Bladder	Bladder	Rectum	Rectum	Small Bowel	Small Bowel		PTV	PTV	PTV	Bladder	Bladder	Rectum	Rectum	Small Bowel	Small Bowel
	Max	Mean	V95	Max	Mean	Max	Mean	Max	Mean		Max	Mean	V95	Max	Mean	Max	Mean	Max	Mean
FX1	0.00	0.00	0.36	0.50	0.20	0.00	−0.10	−0.80	−0.50	FX1	0.20	0.10	−0.04	0.10	−1.00	0.20	0.10	−1.80	−1.90
FX2	−0.10	0.20	0.74	−0.10	−0.10	−0.50	−0.10	−1.60	−0.50	FX2	0.20	0.00	−0.53	0.00	−0.60	0.20	0.00	−0.20	**−4.00**
FX3	0.20	0.10	0.42	0.20	−0.20	−0.10	0.10	−0.80	−0.50	FX3	0.00	−0.10	−0.81	0.00	0.10	−0.30	−0.20	0.10	**−4.20**
FX4	−0.10	0.10	0.79	0.10	−0.10	−0.10	0.10	0.20	−0.30	FX4	0.00	−0.10	−0.60	0.20	0.00	0.10	−0.30	−0.90	**−5.50**
FX5	0.00	0.20	1.00	−0.10	−0.40	−0.10	0.10	0.60	−0.80	FX5	0.30	0.00	−0.23	0.00	0.10	−0.40	−0.30	0.40	**−3.80**
MEAN	0.00	0.12	0.66	0.12	−0.12	−0.16	0.02	−0.48	−0.52	MEAN	0.14	−0.02	−0.44	0.06	−0.28	−0.04	−0.14	−0.48	**−3.88**
ST. DEV	0.12	0.08	0.27	0.25	0.22	0.19	0.11	0.88	0.18	ST. DEV	0.13	0.08	0.31	0.09	0.50	0.29	0.18	0.88	1.29

All differences are as a percentage of the prescription dose, with those greater than 2% shown as boldface.

at risk dosimetric statistics that were similar to an explicit correction strategy. The maximum observed difference across all patients, all structures, and all image-guidance sessions was −5.5% for the small bowel mean dose, for fraction 4 of pelvic patient 6.

To provide better perspective on these results, the same comparisons were also performed for the plans that employed the translations only and zero correction strategies. While only 10 of the 470 metrics investigated disagreed by more than 2% when we compared plans using the virtual corrections with those using the explicit corrections, this number increased to 97 for the translations only corrections and 195 for the zero correction methodology, thus indicating that the virtual correction approach performed significantly better in this regard than either of the commonly available alternatives to

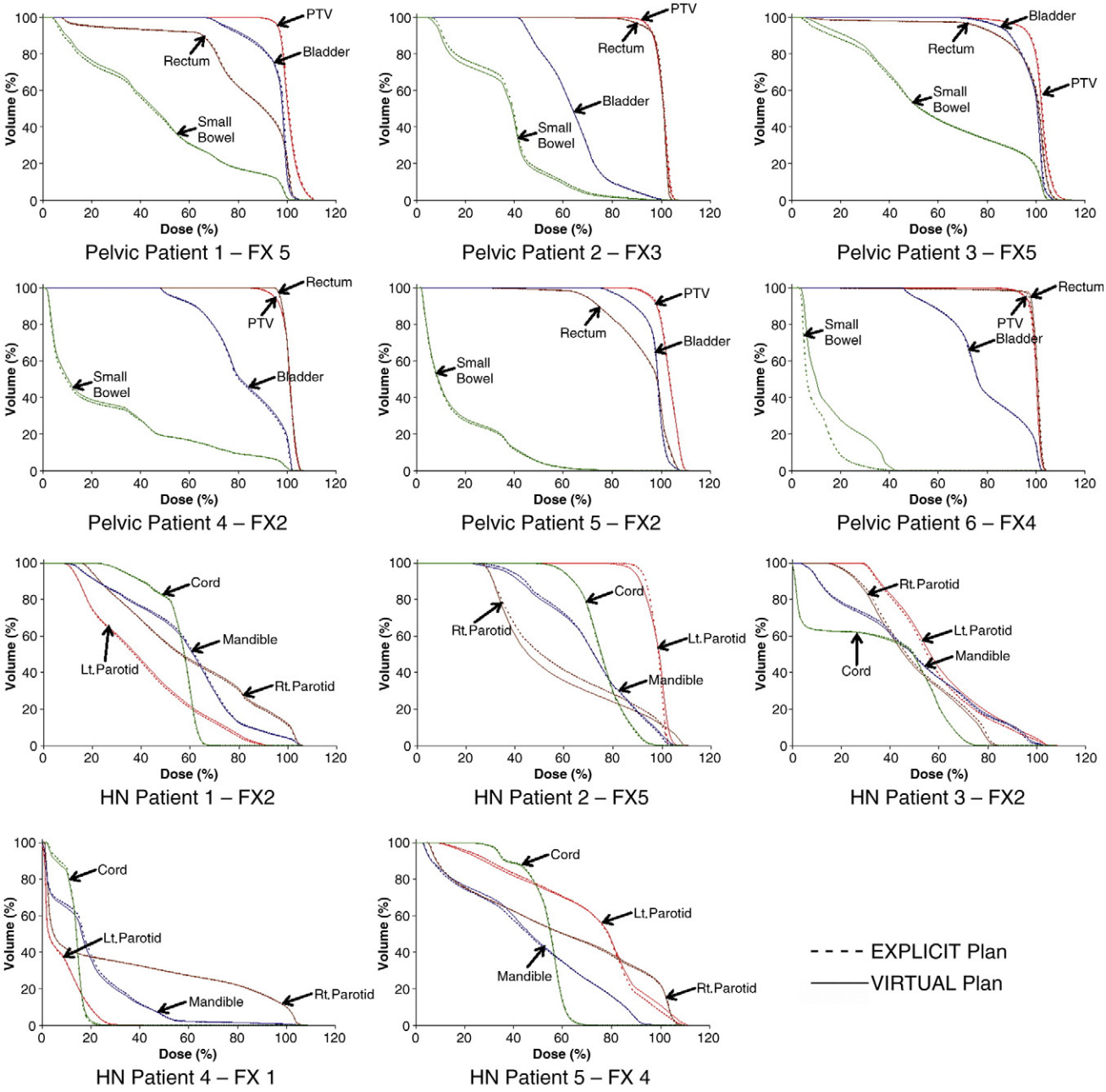

Figure 3 Dose-volume histograms (DVHs) for each patient from the fraction with the "worst" agreement between explicit and virtual corrections. The solid lines show the DVHs from the plan with virtual corrections while dashed lines show DVHs from the plans with explicit corrections. Even for these "worst case" scenarios, the virtual method DVHs can be seen to agree quite well with the explicit method.

robotic correction. Interestingly, the mean percentage dose difference (across all patients and sites) between the translations only and the explicit robotic correction was +0.13%, but the standard deviation was 2.09%; versus the mean percentage difference between virtual and explicit corrections of −0.12% with a standard deviation of only 0.82%. This suggests that the commonly employed translations only approach averages out the errors over multiple fractions, but could result in a relatively large error for any particular fraction. The maximum observed error for the translations only approach was 11.8% (small bowel mean, patient No. 6, fraction No. 4) versus 5.5% for the virtual correction approach. For additional perspective and contrast, the mean percentage dose difference (across all patients and sites) between the zero correction and the explicit robotic correction was worse still, at −0.31%, with a standard deviation of 4.58% (maximum observed error of +21.5%, small bowel mean, patient #6, fraction #4).

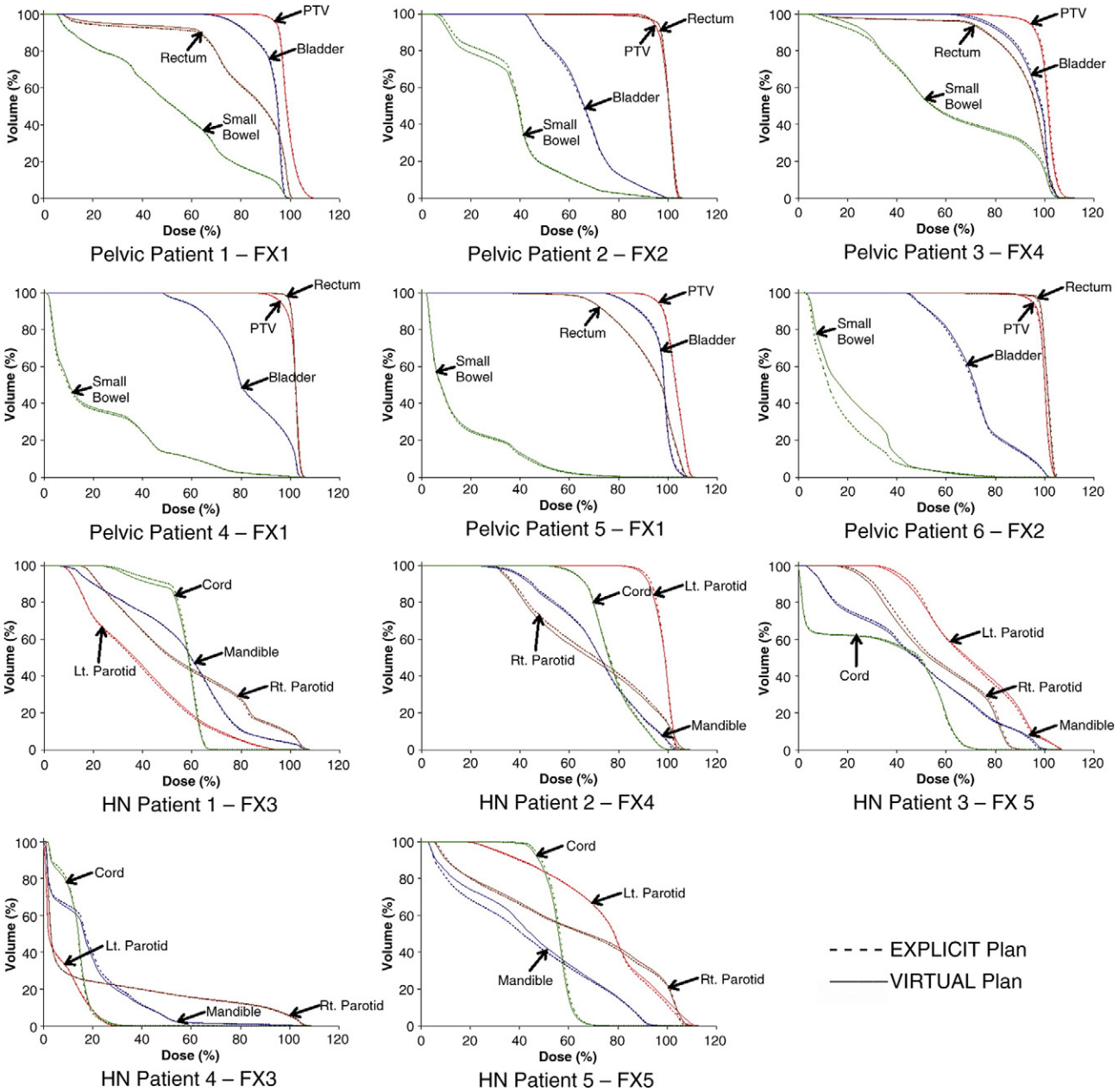

Figure 4 Dose-volume histograms (DVHs) for each patient from the fraction where the agreement between explicit and virtual corrections was the closest to the mean for all fractions (ie, "typical"). The solid lines show the DVHs from the plan with virtual corrections while dashed lines show DVHs from the plans with explicit corrections.

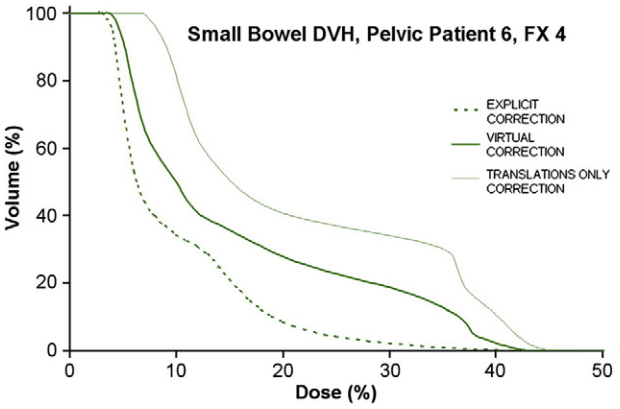

Figure 5 Dose-volume histograms (DVHs) showing the impact of different correction strategies on the small bowel dose for the treatment fraction that showed the worst agreement between plans using the virtual versus explicit corrections. We note that while the virtual plan DVH is not in perfect agreement with the explicit plan for this particular fraction and this particular structure, it still outperforms the translations only plan in terms of agreement with the explicit approach and it yields improved organ sparing relative to the translations only plan.

In order to present a more complete representation of the dose distributions that resulted from each approach, DVHs are presented in Figs 3 and 4. For each patient, the DVHs from the fraction with the worst agreement between explicit and virtual corrections are shown in Fig 3 while Fig 4 depicts DVHs for each patient for the fraction where the agreement was closest to the mean (ie, "typical"). It is clear from the figures that, for even the worst case scenarios, the DVH agreement is still quite good. The largest difference can be seen to have occurred in Fig 3 (ie, the "worst case" figure) for pelvic patient 6, FX4 small bowel, with both the explicit and virtual approaches yielding nearly identical maximum small bowel doses, but with the virtual correction approach yielding somewhat higher volumes at the intermediate to low doses levels. Figure 5 shows an enlarged view of this worst case, pelvic patient 6 FX4 DVH, but with the small bowel results for the translations only correction strategy included for added perspective. This addition makes clear that while there are indeed differences between the virtual and explicit approaches at the intermediate to low dose levels of the small bowel, the virtual correction strategy still significantly outperformed the more commonly employed translations only approach for this structure.

Comparison of corrective strategies using gamma evaluation

Table 6 lists the gamma pass rates for all the comparisons performed with the (2%, 2mm) criteria. Since a higher percentage of points with a gamma value of 1 or less indicates that more points agree within the criteria used, it is clear that the virtual corrective strategy performs better than the translations only and zero corrections strategies in producing dose distributions closer to what would have been achieved had we used an explicit robotic couch approach (mean = 95.1%, 90.4%, 84.7% for virtual, translations only, and zero correction, respectively, for the (2%, 2mm) criteria). We include only the complete results for the relatively stringent (2%, 2mm) gamma criteria here in the interest of space, but the results were similar for all other gamma criteria choices in that the virtual approach outperformed the translations only approach in all cases: mean = 97.3%, 94.4%, 88.8% for virtual, translations only, and zero correction, respectively, for (3%, 3mm) criteria; mean = 91.3%, 86.0%, 81.4% for virtual, translations only, and zero correction, respectively, for (2%, 1mm) criteria; mean = 87.0%, 82.0%, 78.3% for virtual, translations only, and zero correction, respectively, for (1%, 1mm) criteria. For the (2%, 2mm) criteria, the virtual correction method explored here showed mean improvement over the translations only approach of 4.7% ± 3.0%; max = 12.8%, min = 0.1% and came, on average across all cases explored here for the (2%, 2mm) criteria, within 4.9% of an explicit robotic table correction.

Discussion

Daily image-guided correction of patient position and orientation is now common and, for many anatomical sites, considered standard of practice. While most commonly utilized image-guidance approaches are capable of facilitating the calculation of 6DOF corrections, standard linac couches are not currently capable of performing the pitch and roll components of the rotational corrections. Some users have seen fit to invest in hardware upgrades that replace the standard linac couch top with a robotic couch top that is capable of performing all 6DOF corrections. Such upgrades can allow for highly accurate correction of patient position and orientation but require significant investment of capital funding. Bose et al[23] have proposed a virtual approach wherein 6DOF rotational corrections can be implemented through adjustments made to gantry angle, collimator angle, and a single couch yaw rotation, and such an approach is appealing in that it could allow current users of typically equipped linacs to enjoy the ability to "virtually" perform 6DOF corrections.

We note here that Yue et al have previously reported[25] on a method that allows for an exact solution for a 6DOF correction by using a different couch yaw value for each beam, but the strength of the virtual correction methodology explored here, in our opinion, is that a single couch yaw correction is employed, thus realizing the delivery efficiencies afforded by such an approach while simultaneously avoiding the likelihood of gantry or couch collisions.

While Bose et al[23] previously presented a proof of principle clinical example, we believe that, in order to

Table 6 Summary of gamma analysis performed to compare dose distributions from plans generated using the virtual, translations only, and zero correction strategies to the plans using explicit corrections

Case	Gamma criterion (%,mm)	Virtual correction	Translations only	Zero correction
Pelvis 1 Fx 1	2,2	95.58	84.82	82.33
Pelvis 1 Fx 2	2,2	90.06	85.96	76.16
Pelvis 1 Fx 3	2,2	92.54	84.19	77.33
Pelvis 1 Fx 4	2,2	93.21	81.96	67.4
Pelvis 1 Fx 5	2,2	87.61	79.67	79.17
Pelvis 2 Fx 1	2,2	94.93	91.14	90.22
Pelvis 2 Fx 2	2,2	94.11	90.73	87.66
Pelvis 2 Fx 3	2,2	97.38	94.62	86.21
Pelvis 2 Fx 4	2,2	95.5	91.65	91.2
Pelvis 2 Fx 5	2,2	99.37	96.45	90.15
Pelvis 3 Fx 1	2,2	93.19	84.43	79.1
Pelvis 3 Fx 2	2,2	96.37	95.97	80.39
Pelvis 3 Fx 3	2,2	94.59	91.51	85.39
Pelvis 3 Fx 4	2,2	91.34	84.64	79.46
Pelvis 3 Fx 5	2,2	91.97	88.48	78.68
Pelvis 4 Fx 1	2,2	95.56	88.87	76.28
Pelvis 4 Fx 2	2,2	93.72	87.34	74.27
Pelvis 4 Fx 3	2,2	95.29	88.97	75.19
Pelvis 4 Fx 4	2,2	95.51	86.12	81.5
Pelvis 4 Fx 5	2,2	97.48	92.95	79.75
Pelvis 5 Fx 1	2,2	87.91	79.69	67.98
Pelvis 5 Fx 2	2,2	92.43	84.3	72.47
Pelvis 5 Fx 3	2,2	92.74	86.29	74.25
Pelvis 5 Fx 4	2,2	93.68	83.31	74.5
Pelvis 5 Fx 5	2,2	90.99	83.17	69.51
Pelvis 6 Fx 1	2,2	93.08	90.11	77.25
Pelvis 6 Fx 2	2,2	89.55	84.26	79.38
Pelvis 6 Fx 3	2,2	88.36	84.74	81.08
Pelvis 6 Fx 4	2,2	87.3	81.68	75.91
Pelvis 6 Fx 5	2,2	90.52	85.36	80.04
H&N 1 Fx 1	2,2	96.72	96.64	85.93
H&N 1 Fx 2	2,2	98.9	86.11	81.72
H&N 1 Fx 3	2,2	96.66	94.14	85.3
H&N 1 Fx 4	2,2	96.04	93.03	84.86
H&N 1 Fx 5	2,2	97.9	93.67	87.46
H&N 2 Fx 1	2,2	97.19	91.51	91.53
H&N 2 Fx 2	2,2	97.34	91.37	92.77
H&N 2 Fx 3	2,2	97.31	94.41	90.19
H&N 2 Fx 4	2,2	95.64	91.74	93.89
H&N 2 Fx 5	2,2	91.51	87.68	86.86
H&N 3 Fx 1	2,2	98.95	98.36	95.19
H&N 3 Fx 2	2,2	99.22	97.8	97.02
H&N 3 Fx 3	2,2	99.09	97.45	97.03
H&N 3 Fx 4	2,2	99.17	98.92	95.89
H&N 3 Fx 5	2,2	99.12	98.58	96.48
H&N 4 Fx 1	2,2	98.86	97.17	96.2
H&N 4 Fx 2	2,2	98.54	96.19	93.99
H&N 4 Fx 3	2,2	99	96.93	96.26
H&N 4 Fx 4	2,2	99.37	95.39	93.57
H&N 4 Fx 5	2,2	98.65	95.87	94.43
H&N 5 Fx 1	2,2	95.88	91.53	89.42
H&N 5 Fx 2	2,2	95.73	90.17	89.45
H&N 5 Fx 3	2,2	96.43	93.32	89.75
H&N 5 Fx 4	2,2	97.93	95.27	94.28
H&N 5 Fx 5	2,2	96.29	94.27	89.71
Average		95.1	90.4	84.7
Std. Deviation		3.4	5.4	8.3

H&N, head and neck.

rigorously determine the clinical viability of such an approach, a large number of image-guided sessions must be evaluated to more completely encompass the numerous geometric scenarios that can be encountered clinically. Here we evaluated 55 different image-guided sessions for 11 different patients with either H&N or pelvic disease sites and we investigated 5 different image-guided datasets for each patient.

It is also important, we believe, that such an evaluation utilizes high-quality CT images so that undesired variation in organ delineation is not introduced as a result of reduced image quality, and so that highly accurate dose calculation is facilitated. It remains questionable as to whether or not current generation, on-board cone beam CT imaging systems are capable of providing such image quality. Fortunately, for this work we were able to utilize diagnostic quality fan beam CT images obtained from the in-room CTOR unit we routinely use for image-guided alignment of conformally treated patients in our clinic. By utilizing such high-quality image sets we ensured both the accuracy of calculated dose distributions and that relevant structures were delineated on image-guidance CT image sets that were of equivalent quality to the original CT simulation datasets. Additionally, we took care to require that the physician who contoured the relevant structures on the CT simulation dataset also contoured the structures on the CTOR "image sets of the day."

It is clear from data presented in Figs 1 and 2 and Table 3 that geometric comparison of fiducial locations yielded very similar results for the virtual correction approach when compared with the explicit approach. Results for the 2 worst cases observed (of 55 total), for fiducial locations intentionally chosen at the field edge so as to maximize the manifestation of rotationally induced translational errors, still yielded fiducial-to-beam coordinates that were within 3 mm of an explicit robotic correction approach (mean = 2.2 mm and 1.0 mm for the pelvis and H&N, worst case cases, respectively [max = 3.0 mm and 1.0 mm, respectively]).

Similarly, when comparison of dosimetric statistics and DVHs for the virtual correction approach and the explicit robotic correction strategy was performed, Tables 4 and 5 and Figs 3 and 4 show that the virtual correction approach achieved essentially equivalent results to those calculated for an explicit robotic correction approach. Of the 470 maximum or mean data statistics collected across all patients and relevant structures, only 10 values exceeded a 2% difference between the 2 methods. Mean difference across all alignments, across all patients, was −0.12% with a standard deviation of 0.82%; again indicating that the virtual correction approach was essentially equivalent to the explicit robotic approach for the 55 image-guided sessions studied here.

Finally, we performed an extensive gamma analysis comparison of the dose distributions achieved when employing the virtual correction approach, relative to that achieved when employing an explicit robotic correction. The gamma analysis results are, in our opinion, particularly notable in that such analysis compared all calculated dose points above the 10% dose level and, as such, represent a very thorough characterization of the degree of agreement between the virtual and explicit approaches. In particular, we note that for all gamma analysis scenarios evaluated here (ie, (3%, 3mm), (2%, 2mm), (2%, 1mm), and (1%, 1mm)), the virtual correction approach significantly outperformed the most commonly employed clinical strategy of translations only. For the (2%, 2mm) criteria results presented in Table 6, the improvement averaged 4.7% ± 3%, and for this same (2%, 2mm) criteria the virtual approach came, on average, across all 55 cases explored here, within 4.9% of reproducing the dosimetric results of an explicit robotic correction. We note that this level of agreement is comparable with levels of agreement generally considered as clinically acceptable when comparing intensity modulated delivered dose distributions with intended dose distributions (eg, 95%), but for the much less stringent (3%, 3mm) criteria.

In summary, the virtual correction approach investigated here was seen (for 11 different patients, 55 different H&N and pelvic image-guided sessions) to yield both geometric and dosimetric results that consistently and significantly outperformed the most commonly employed alternative strategy (translations only), and to produce gamma analysis agreement for a very stringent (2%, 2mm) criteria that averaged over 95% agreement with a robotically implemented explicit correction approach.

Conclusions

A virtual image-guidance correction method which utilizes beam-specific gantry and collimator rotations along with a single couch yaw rotation to correct for patient pitch, roll and yaw rotations was compared with the gold standard robotic couch explicit correction method. Geometric analysis of fiducial points for both methods were compared and the virtual correction approach was seen to yield a worst case, maximum deviation from explicit robotic result of 3 mm (mean = 2.2 mm and 1.0 mm for the pelvis and H&N, worst case cases, respectively) and to outperform the commonly used translations only approach in all cases. Calculated dose distributions using each of the 2 methods were compared by DVH analysis and dose statistics (such as maximum and mean structure doses) and the virtual approach was seen to perform, on average, within −0.12% ± 0.82% of the explicit robotic approach and, again, to consistently outperform the most commonly employed clinical approach of translations only.

Finally, gamma analysis comparison, identical to that commonly used to compare "intended" IMRT dose

distributions to "delivered" IMRT dose distributions, again showed that the virtual correction approach significantly outperformed the most commonly employed clinical strategy of translations only. For a very stringent (2%, 2mm) gamma criteria the improvement averaged 4.7% ± 3%, and for the same (2%, 2mm) criteria the virtual approach yielded, on average, across all 55 cases explored here; over 95% dosimetric agreement relative to an explicit robotic table correction. As such, the method appears to represent a clinically viable and potentially significant opportunity for typical linac users to avail themselves of 6DOF correction capability without the requirement to upgrade to robotic couch top technology.

References

1. Lattanzi J, McNeeley S, Donnelly S, et al. Ultrasound-based stereotactic guidance in prostate cancer–quantification of organ motion and set-up errors in external beam radiation therapy. *Comput Aided Surg.* 2000;5:289-295.
2. Geinitz H, Zimmermann FB, Kuzmany A, Kneschaurek P. Daily CT planning during boost irradiation of prostate cancer. Feasibility and time requirements. *Strahlenther Onkol.* 2000;176:429-432.
3. Weiss E, Vorwerk H, Richter S, Hess CF. Interfractional and intrafractional accuracy during radiotherapy of gynecologic carcinomas: a comprehensive evaluation using the ExacTrac system. *Int J Radiat Oncol Biol Phys.* 2003;56:69-79.
4. Wong JR, Cheng CW, Grimm L, Uematsu M. Clinical implementation of the world's first primatom, a combination of CT scanner and linear accelerator, for precise tumor targeting and treatment. *Physica Medica.* 2001;17:271-276.
5. Shiu AS, Chang EL, Ye JS, et al. Near simultaneous computed tomography image-guided stereotactic spinal radiotherapy: an emerging paradigm for achieving true stereotaxy. *Int J Radiat Oncol Biol Phys.* 2003;57:605-613.
6. Ma CM, Paskalev K. In-room CT techniques for image-guided radiation therapy. *Med Dosim.* 2006;31:30-39.
7. Ahunbay EE, Peng C, Holmes S, Godley A, Lawton C, Li XA. Online adaptive replanning method for prostate radiotherapy. *Int J Radiat Oncol Biol Phys.* 2010;77:1561-1572.
8. Siewerdsen JH, Jaffray DA. A ghost story: spatio-temporal response characteristics of an indirect-detection flat-panel imager. *Med Phys.* 1999;26:1624-1641.
9. Siewerdsen JH, Jaffray DA. Cone-beam computed tomography with a flat-panel imager: effects of image lag. *Med Phys.* 1999;26: 2635-2647.
10. Jaffray DA, Siewerdsen JH. Cone-beam computed tomography with a flat-panel imager: initial performance characterization. *Med Phys.* 2000;27:1311-1323.
11. Siewerdsen JH, Jaffray DA. Cone-beam computed tomography with a flat-panel imager: magnitude and effects of x-ray scatter. *Med Phys.* 2001;28:220-231.
12. McBain CA, Henry AM, Sykes J, et al. X-ray volumetric imaging in image-guided radiotherapy: the new standard in on-treatment imaging. *Int J Radiat Oncol Biol Phys.* 2006;64:625-634.
13. Sorcini B, Tilikidis A. Clinical application of image-guided radiotherapy, IGRT (on the Varian OBI platform). *Cancer Radiother.* 2006;10:252-257.
14. Gayou O, Miften M. Commissioning and clinical implementation of a mega-voltage cone beam CT system for treatment localization. *Med Phys.* 2007;34:3183-3192.
15. Song WY, Kamath S, Ozawa S, et al. A dose comparison study between XVI and OBI CBCT systems. *Med Phys.* 2008;35:480-486.
16. Bert C, Metheany KG, Doppke K, Chen GT. A phantom evaluation of a stereo-vision surface imaging system for radiotherapy patient setup. *Med Phys.* 2005;32:2753-2762.
17. Balter JM, Wright JN, Newell LJ, et al. Accuracy of a wireless localization system for radiotherapy. *Int J Radiat Oncol Biol Phys.* 2005;61:933-937.
18. Su Z, Zhang L, Murphy M, Williamson J. Analysis of prostate patient setup and tracking data: potential intervention strategies [published online ahead of print October 8, 2010]. *Int J Radiat Oncol Biol Phys.* doi:10.1016/j.ijrobp.2010.07.1978.
19. Tanyi JA, He T, Summers PA, et al. Assessment of planning target volume margins for intensity-modulated radiotherapy of the prostate gland: role of daily inter- and intrafraction motion. *Int J Radiat Oncol Biol Phys.* 2010;78:1579-1585.
20. Guckenberger M, Meyer J, Wilbert J, Baier K, Sauer O, Flentje M. Precision of image-guided radiotherapy (IGRT) in six degrees of freedom and limitations in clinical practice. *Strahlenther Onkol.* 2007;183:307-313.
21. Takakura T, Mizowaki T, Nakata M, et al. The geometric accuracy of frameless stereotactic radiosurgery using a 6D robotic couch system. *Phys Med Biol.* 2010;55:1-10.
22. Wilbert J, Meyer J, Baier K, et al. Tumor tracking and motion compensation with an adaptive tumor tracking system (ATTS): system description and prototype testing. *Med Phys.* 2008;35:3911-3921.
23. Bose S, Shukla H, Maltz J. Beam-centric algorithm for pretreatment patient position correction in external beam radiation therapy. *Med Phys.* 2010;37:2004-2016.
24. Low DA, Harms WB, Mutic S, Purdy JA. A technique for the quantitative evaluation of dose distributions. *Med Phys.* 1998;25: 656-661.
25. Yue NJ, Knisely JP, Song H, Nath R. A method to implement full six-degree target shift corrections for rigid body in image-guided radiotherapy. *Med Phys.* 2006;33:21-31.